PHYSICAL REVIEW B **77**, 081401(R) (2008)

Formation of single- and double-layer silicon in slit pores

Tetsuya Morishita,* Kengo Nishio, and Masuhiro Mikami
Research Institute for Computational Sciences (RICS), National Institute of Advanced Industrial Science and Technology (AIST), 1-1-1 Umezono, Tsukuba, Ibaraki 305-8568, Japan
(Received 22 October 2007; published 6 February 2008)

We report on the formation of quasi-two-dimensional nanostructures of silicon by quenching liquid silicon confined in slit nanopores. The formation processes are investigated by molecular-dynamics (MD) calculations using the Tersoff potential. We find that single- or double-layer nanosheets are formed according to the slit width. Both of these nanosheets contain hexagonal planes, and the structure of the single-layer nanosheet is the same as that of graphene. The stability of these nanosheets within the slit nanopore is confirmed by first-principles MD calculations up to 300 K. The present findings demonstrate the possibility of the synthesis of novel nanostructures by confinement in nanopores.

DOI: 10.1103/PhysRevB.77.081401 PACS number(s): 81.07.−b, 61.46.−w, 71.15.Pd, 81.16.Dn

The fabrication of nanoscale materials has been a topic of intense research for the past decades. Since the discovery of carbon nanotubes by Iijima,[1] nanoscale forms in a variety of materials have been explored in experiments and numerical calculations.[2–8] In particular, silicon (Si) nanoforms, such as nanotubes (NTs), nanowires, and nanosheets, have been a focus of growing interest due to their potential technological applications.[9–16] One of the appealing features of such low-dimensional structures is the quantum confinement effect, which is able to alter energy band structures. Many attempts have thus been made to design novel electronic devices based on these Si nanoforms.[2,3]

Exploiting nanopores is a promising way to produce low-dimensional nanoscale materials. A molecular-dynamics (MD) study by Koga *et al.* has demonstrated that water confined in a *cylindrical* nanopore crystallizes into ice NTs.[6] The characteristics of these ice NTs strongly depend on the diameter of the nanopores: square, pentagonal, and hexagonal ice NTs have been formed according to the diameter of the nanopore.[6] It has also been demonstrated that quasi-two-dimensional (quasi-2D) crystal or amorphous ice can be formed in *slit* nanopores.[7,8] These quasi-2D ices contain layered structures in which hydrogen bonds are preserved as in a bulk ice.

Similar to confined water, liquid Si (*l*-Si) in nanopores also exhibits phase transitions to low-dimensional crystalline structures. The formation of single-walled Si NTs from *l*-Si in a cylindrical nanopore has recently been demonstrated[14] by MD calculations using the Stillinger-Weber potential. The structures of these Si NTs are different from the structure of a single-walled carbon NT; they are rather similar to those of ice NTs mentioned above. It has also been reported that the Tersoff potential[17] yields Si nanowires consisting of icosahedral structures in cylindrical nanopores.[15] However, despite much work on such quasi-1D Si nanostructures, knowledge of 2D Si nanostructures is currently lacking. Two-dimensional nanoforms of Si are in fact potential candidate materials for field-effect transistors with thin channel layers, these transistors being one of the key devices in nanoscale technology. It is therefore a matter of great interest to explore possible 2D Si nanostructures.

In this Rapid Communication, we demonstrate the formation of 2D layered structures of Si in slit nanopores by MD calculations using the Tersoff potential. According to the slit width, single-or double-layer structures have been formed by quenching a confined *l*-Si. The stability of these layered structures has been further confirmed by first-principles MD (FPMD) calculations, which strongly support the existence of these layered Si nanosheets.

We performed MD simulations of Si atoms confined between two parallel-plane walls that act as chemically inert confinement for the Si atoms. The interaction between Si atoms was described by the Tersoff potential.[17] It is known that the Tersoff potential provides an accurate description of a high-pressure polymorph of Si (Ref. 18) as well as liquid and amorphous states at normal pressure, which is helpful in simulating the confined Si system as shown later. Each atom also interacts with the slit walls via the 9-3 Lennard-Jones (LJ) potential.[19] The LJ parameters for the Si-wall interaction were calculated by the Lorenz-Berthelot combining rule: $\sigma_{12}=\sigma_1+\sigma_2=3.74$ Å and $\varepsilon_{12}=\sqrt{\varepsilon_1\varepsilon_2}=8.2125\times10^{-2}$ eV, where σ_1 and ε_1 are the LJ parameters for graphite and σ_2 and ε_2 are those for the SiH_4 molecule.[20] Our preliminary calculations of Si in cylindrical nanopores have shown that both structureless and realistic structured walls (carbon NTs) yield essentially the same results.[15,21] Materials such as layered oxides and graphite can be considered potential candidates for the actual slit wall.[22]

Liquid Si consisting of 512 Tersoff atoms was first prepared in the slit nanopore of width $h_z=9.3$ Å with free boundary conditions (in the x and y directions). This confined *l*-Si was equilibrated for ~1 ns at 2400 K and was then quenched down to 0 K at a rate of 2×10^{10} K/s (10 K per 500 ps) by velocity scaling. In this quenching process, a layered structure was formed in the slit nanopore. Similar procedures were followed to perform subsequent MD runs with different slit widths ($h_z=6.5-13$ Å). Some of these MD runs employed 2D periodic boundary conditions (in the x and y directions) and a quench rate of 1×10^{10} K/s, but such detailed conditions did not exert a significant influence on the formation of the layered structures. For the layered structures obtained in the Tersoff MD simulations, FPMD calculations based on plane-wave density functional theory (DFT) were performed to examine their stability. The unit structures con-

taining 32 or 64 atoms were extracted from the obtained layered structures in the Tersoff MD simulations and were arranged in a supercell with periodic boundary conditions.[23] FPMD runs were then initiated at constant volume (fixed area density and slit width), and the stability in the slit nanopore was confirmed up to 300 K. Considering that the whole formation process cannot be simulated by FPMD due to its heavy computation, a combination of empirical MD and FPMD appears promising for exploring novel nanostructures in computer simulations.

The temperature dependence of the potential energy per atom, U, in the quenching process for the confined system with 512 Tersoff atoms is shown in Fig. 1(a). We clearly see that U exhibits a sharp drop at ~1700 K, suggesting a first-order transition from a liquid to a solid state. The temperature dependence of the atomic mobility also supports the occurrence of the liquid-solid transition. The root-mean-square displacement (RMSD) parallel to the wall during 10 ps was calculated for each atom, which was then averaged over atoms and 50 time origins at each temperature. The inset of Fig. 1(a) shows the temperature dependence of the 2D RMSD. A sharp drop is again seen at ~1700 K and the RMSD is less than 1 Å at temperatures <1700 K. Solidification at ~1700 K therefore is manifest. We have confirmed that the RMSD perpendicular to the wall (not shown) also exhibits a sharp drop at ~1700 K.

The 2D radial distribution function $g(r_{xy})$ is given in Fig. 1(b). At 2400 K, the first peak is found at ~2.35 Å, but the second and third peaks are much broader than the first peak. In contrast, $g(r_{xy})$ at temperatures ≤400 K indicates that a crystalline ordering is formed in the confined system.

The number density profile perpendicular to the wall also confirms the liquid-crystal transition [Fig. 1(c)]. A broad distribution with two visible peaks (~3 and ~6 Å) is seen at 2400 K. These two peaks grow in intensity and split into two subpeaks upon quenching to 400 K. The distribution between 3.8 and 5.5 Å disappears at 400 K, indicating the formation of a double-layer structure.

Atomic configurations (quenched to 0 K) of the double-layer structure thus obtained are displayed in Figs. 2(a) and 2(b). It is clearly shown that the (0001) plane of the hexagonal diamond structure is formed in parallel to the walls. This structure is similar to that of double-layer TIP4P ice.[7] Viewed from the [0001] direction (perpendicular to the walls), all atoms in the upper layer are stacked onto the atoms in the lower layer, in contrast to those in the (111) plane of the cubic diamond structure in which one atom in the lower hexagonal layer is found in the middle of each hexagon in the upper layer. The average length of the inplane bond is 2.33 Å and that of the interplane bond is 2.36 Å. These two bond lengths should be equal in the bulk diamond structure. The tetrahedra in this double-layer Si are thus slightly distorted.

In contrast to the bulk crystal Si, which possesses cubic diamond (CD) structure, the double-layer Si formed in our simulations contains the hexagonal diamond (HD) structure only. To gain further insight into the formation of the double-layer structure, local atomic configurations in the confined l-Si were carefully examined. Figure 2(c) shows a local atomic configuration peculiar to the confined l-Si. As can be seen, four-membered rings (rectangular configurations) are formed parallel or perpendicular to the slit walls. In particular, the formation of the four-membered rings perpendicular to the walls [red atoms in Fig. 2(c)] appears to play a key

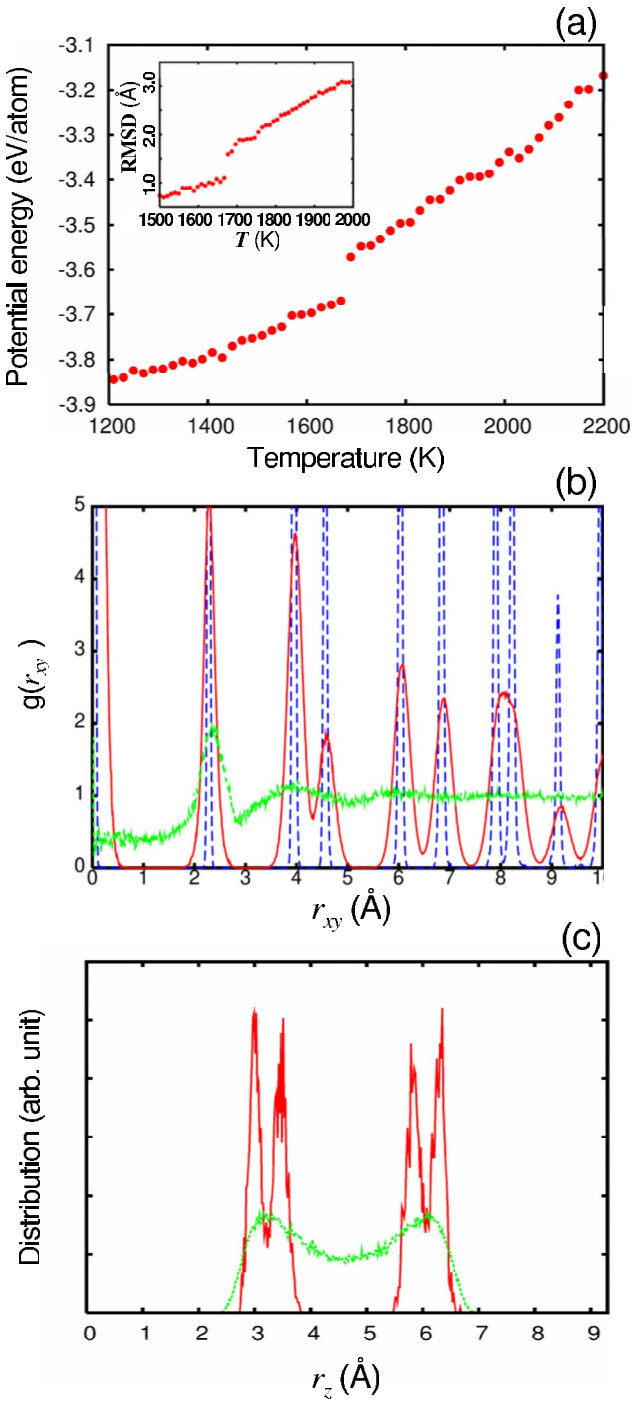

FIG. 1. (Color online) (a) Temperature dependence of the potential energy per atom for the Tersoff Si in the slit nanopore of h_z=9.3 Å (the Si-wall interactions is excluded). Inset: temperature dependence of 2D RMSD during 10 ps. (b) 2D radial distribution function for the confined Tersoff Si at 20 K (dashed lines), 400 K (solid lines), and 2400 K (dotted lines). (c) Distribution of the number density in the z direction (perpendicular to the walls) for the confined Tersoff Si at 400 K (solid lines) and 2400 K (dotted lines).

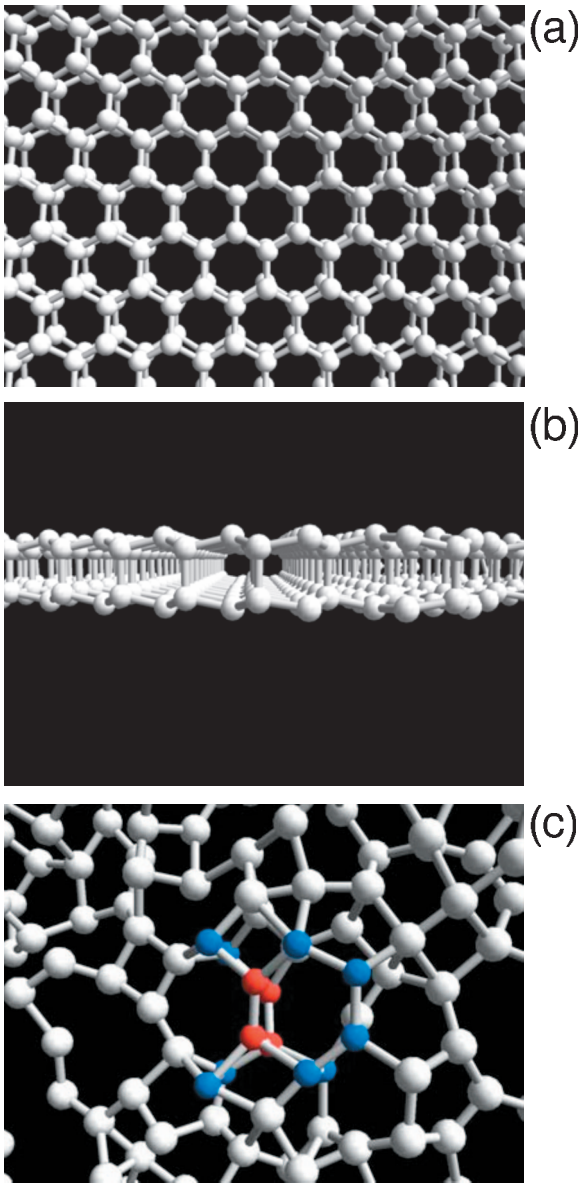

FIG. 2. (Color) Structures of the confined Tersoff Si (displayed in perspective). (a) Top view and (b) side view of the double-layer Si confined in the slit nanopore of h_z=9.3 Å. (c) A local atomic configuration in the confined *l*-Si viewed from the *z* direction (perpendicular to the walls). A fragment of the HD layer (blue and red atoms) is formed parallel to the walls, and a four-membered ring (red atoms) is formed perpendicular to the walls.

role in the formation of the HD structure. Owing to the confined space, tetrahedral structures are slightly distorted, and thus, atomic bonds tend to form rectangular configurations that are typically formed in high-pressure polymorphs of Si.[26] Once such rectangles are formed perpendicular to the walls, a fragment of the HD structure is easily constructed due to the geometrical restriction of (distorted) tetrahedral bonds as shown in Fig. 2(c). It is therefore considered that the double-layer Si with HD structure is more easily formed than that with CD structure in the slit nanopore of $h_z \sim 9$ Å. We should remark here that, using the Tersoff potential, both the HD and CD structures have exactly the same structural

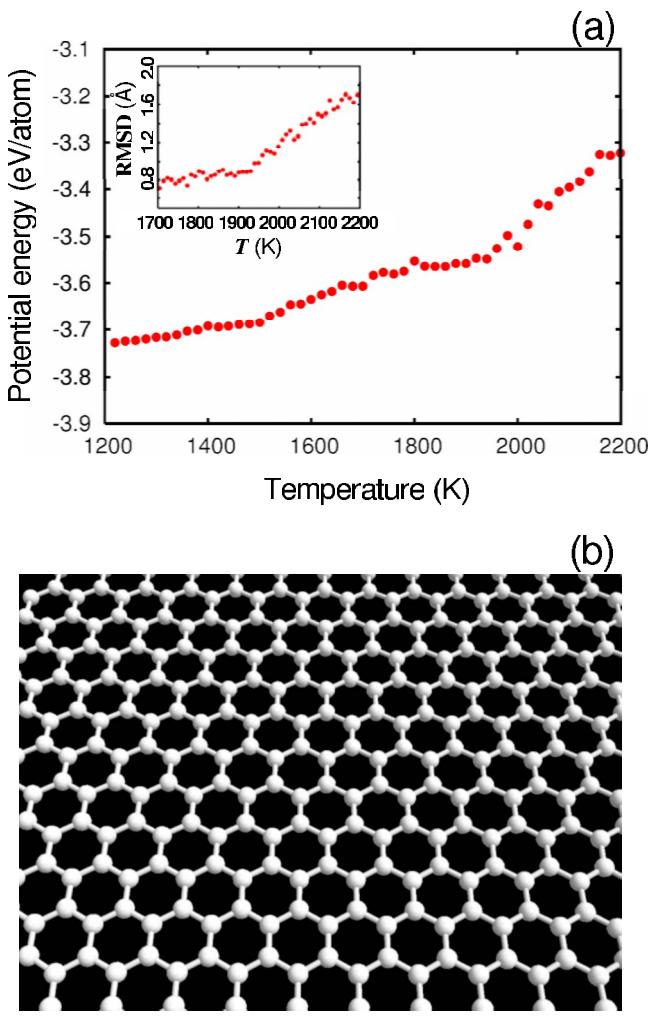

FIG. 3. (Color online) (a) Temperature dependence of the potential energy per atom for the Tersoff Si in the slit nanopore of h_z=6.5 Å (the Si-wall interactions is excluded). Inset: temperature dependence of 2D RMSD. (b) Structure of the single-layer Si confined in the slit nanopore of h_z=6.5 Å.

energy (U), although the latter has never been formed in double-layer Si. We therefore consider that the HD structure is formed because of the kinetic effect that is significantly influenced by the confinement. In fact, we found triple-layer structures having CD structure as well as HD structure in the case of $h_z \geqslant 12$ Å (the formation of triple-layer Si will be discussed elsewhere).

We have obtained double-layer Si in the slit nanopore of h_z=9.0–11.0 Å. However, in the case of $h_z \leqslant 7.5$ Å, the formation of the double-layer structure has never been observed due to insufficient space. Instead, a single-layer structure has been formed in our calculations. Figure 3(a) shows the temperature dependence of U for the Tersoff *l*-Si in the slit nanopore of h_z=6.5 Å. In contrast to the confined system of h_z=9.3 Å [Fig. 1(a)], U exhibits a gradual change upon quenching. Our visual inspection reveals that the system is almost in a solid state below ~2000 K, while it remains in a liquid state above ~2000 K. In fact, the 2D RMSD (parallel to the wall) during 10 ps is less than 1 Å at temperatures

<2000 K [inset of Fig. 3(a); see also Fig. 1(a)], although its variation is continuous. It should be remarked that the previous MD calculation has demonstrated that TIP4P water confined in a cylindrical nanopore also exhibits continuous transitions from a liquid to an ice NT according to external pressure.[6] The fact that continuous transitions from a liquid to a crystalline phase are observed according to external conditions appears to be peculiar to confined (low-dimensional) systems.

The atomic configuration of the single-layer Si thus obtained is displayed in Fig. 3(b). This single layer is, as can be seen, a flat hexagonal layer. The single-layer Si therefore possesses the same structure as that of graphene. The average bond length is 2.31 Å and the bond angle is, needless to say, 120°. It is demonstrated that the formation of layered structures can be controlled—i.e., the number of hexagonal layers—by adjusting the slit width.

The stability of the single- and double-layer Si within the slit nanopore was further examined by FPMD calculations. Using the steepest-descent algorithm with Hellmann-Feynman forces based on plane-wave DFT, the single-layer (32-atom) and double-layer (64-atom) structures were optimized in the slit nanopore of h_z=6.5 and 9.0 Å, respectively. In this optimization process, the hexagonal layer of the double-layer Si became flatter, but apart from this, no significant structural change occurred. FPMD simulations were then performed for the optimized structures at 300 K. Each atom vibrates around its original lattice position and no structural transformation was observed. Our FPMD calculations thus provide convincing evidence that both of these layered structures are stable in the slit nanopores.

In summary, we have demonstrated the formation of single- and double-layer nanosheets of Si in slit nanopores. The layered structures obtained have not previously been observed in any nanoforms of Si. It is therefore expected that new properties or functions will be exhibited in these layered Si, especially in single-layer Si whose structure is the same as that of graphene. It is worth noting that layered-Si-rich transition-metal silicide has recently been proposed,[16] which may be highly relevant to the layered Si obtained in our calculations. The present findings suggest that controlling the formation of nanostructures is possible by exploiting self-organized formation in confined systems such as slit pores. The novel Si nanostructures obtained in our calculations definitely open new venues for future research regarding electronic and optical nanodevices.

We thank T. Ikeshoji for a careful reading of the manuscript. This work was supported in part by the Next Generation Super Computing Project, the Nanoscience Program. T.M. acknowledges partial support from a Grant-in-Aid for Scientific Research from the Ministry of Education, Culture, Sports, Science and Technology, Japan. The computations were carried out at the Research Center for Computational Science, National Institute of Natural Sciences.

*t-morishita@aist.go.jp

[1] S. Iijima, Nature (London) **354**, 56 (1991).
[2] D. Appell, Nature (London) **419**, 553 (2002).
[3] Y. Cui and C. M. Lieber, Science **291**, 851 (2001).
[4] A. K. Geim and K. S. Novoselov, Nat. Mater. **6**, 183 (2007).
[5] G. Seifert and E. Hernández, Chem. Phys. Lett. **318**, 355 (2000).
[6] K. Koga, G. T. Gao, H. Tanaka, and X. C. Zeng, Nature (London) **412**, 802 (2001).
[7] K. Koga, X. C. Zeng, and H. Tanaka, Phys. Rev. Lett. **79**, 5262 (1997).
[8] R. Zangi and A. E. Mark, Phys. Rev. Lett. **91**, 025502 (2003).
[9] M. Menon and E. Richter, Phys. Rev. Lett. **83**, 792 (1999).
[10] A. S. Barnard and S. P. Russo, J. Phys. Chem. B **107**, 7577 (2003).
[11] I. Ponomareva, M. Menon, D. Srivastava, and A. N. Andriotis, Phys. Rev. Lett. **95**, 265502 (2005).
[12] N. Wang, B. D. Yao, Y. F. Chan, and X. Y. Zhang, Nano Lett. **3**, 475 (2003).
[13] S. Yamada and H. Fujiki, Jpn. J. Appl. Phys., Part 2 **45**, L837 (2006).
[14] J. Bai, X. C. Zeng, H. Tanaka, and J. Y. Zeng, Proc. Natl. Acad. Sci. U.S.A. **101**, 2664 (2004).
[15] K. Nishio, T. Morishita, W. Shinoda, and M. Mikami, J. Chem. Phys. **125**, 074712 (2006).
[16] T. Miyazaki and T. Kanayama, Jpn. J. Appl. Phys., Part 2 **46**, L28 (2007); Appl. Phys. Lett. **91**, 082107 (2007).
[17] J. Tersoff, Phys. Rev. B **39**, R5566 (1989).
[18] K. Mizushima, S. Yip, and E. Kaxiras, Phys. Rev. B **50**, 14952 (1994); I.-H. Lee, J.-W. Jeong, and K. J. Chang, *ibid.* **55**, 5689 (1997).
[19] C. Alba-Simionesco *et al.*, J. Phys.: Condens. Matter **18**, R15 (2006), and references therein.
[20] Y. Sakiyama, S. Takagi, and Y. Matsumoto, Phys. Fluids **16**, 1620 (2004).
[21] K. Nishio, T. Morishita, and M. Mikami (unpublished).
[22] It is worth noting that the interlayer distance of graphite can vary according to intercalated substances. Alkali metals, for instance, intercalated into graphite have been extensively investigated: A. Charlier, M. F. Charlier, and D. Fristot, J. Phys. Chem. Solids **50**, 987 (1989).
[23] The electronic-state calculation was performed within the the local density approximation of DFT. The electronic wave functions were expanded in a plane-wave basis with an energy cutoff of ~17 Ry, and the norm-conserving pseudopotential was used to describe the electron-ion interaction. The details are the same as those in the previous FPMD simulations of liquid and amorphous Si (Refs. 24 and 25). The supercell is a rectangular parallelepiped with dimensions $14.07\times16.0\times14.3$ Å^3. The Si-wall interaction was described by the 9-3 LJ potential similarly to that in the Tersoff Si system.
[24] T. Morishita, Phys. Rev. Lett. **97**, 165502 (2006); Phys. Rev. E **72**, 021201 (2005).
[25] T. Morishita, Phys. Rev. Lett. **93**, 055503 (2004).
[26] A. Mujica, A. Rubio, A. Muñoz, and R. J. Needs, Rev. Mod. Phys. **75**, 863 (2003).